Adhesion Factor of Large Diameter Bored Piles in Soft to Stiff Clay in the Sei Alalak Bridge Replacement Project–South Kalimantan, Indonesia

by Arifin Yulian F

SSRG International Journal of Civil Engineering
ISSN: 2348 – 8352 /doi:10.14445/23488352/IJCE-V8I6P105 Volume 8 Issue 6, 38-47, June 2021

Adhesion Factor of Large Diameter Bored Piles in Soft to Stiff Clay in the Sei Alalak Bridge Replacement Project–South Kalimantan, Indonesia

Andika Mulrosha[1], Yulian Firmana Arifin[2]

[1] *Civil Engineering Master Program, University of Lambung Mangkurat, Banjarmasin, Indonesia*
[2] *Engineer Profession Education, University of Lambung Mangkurat, Banjarbaru, Indonesia*

Received Date: 09 May 2021
Revised Date: 11 June 2021
Accepted Date: 22 June 2021

***Abstract* -** *The purpose of this research was to determine the adhesion factors of soft to stiff clay using both analytical and numerical methods. The data used was from the Sei Alalak Bridge Replacement Project in Banjarmasin, South Kalimantan, which included a field investigation of the bi-directional loading test. The result was analysed using Davisson and Chin methods to obtain the bearing capacity of the pile. Furthermore, the disturbed and undisturbed sample data were used as drilling results at points BH-04 in the bridge's pylon structure. Using field tests and soil data, the adhesion factor was back-calculated using empirical equations proposed by some researchers. Moreover, Plaxis 2D was used in the numerical analysis model. The average adhesion factors in the sub-layers calculated from these two points are 0.943 in the upward position and 0.191 in the downward position at B7. The adhesion factors obtained are very similar to Kulhaway and Jackson's data (1989). Furthermore, PLAXIS 2D Modeling produces adhesion factors of 0.97 and 0.94 in very soft clay and soft clay layers, respectively, while 0.56 and 0.48 in stiff clay and very stiff clay. These adhesion factor distributions resemble those reported by Kulhawy and Jackson (1989) and Coduto (1989).*

Keywords: *bored pile, adhesion factor, shear strength, finite element method, PLAXIS 2D*

I. INTRODUCTION

The 850–meter–long Sei Alalak Bridge was built in three sections: an access road in the form of a road network with a soft pavement structure, a piled slab structure, and a cable–stayed single pylon structure on the bridge's main span. The main span of the Sei Alalak Bridge has 52 bored piles, which are divided into 32 points on the pylon, 12 points on the counterweight, and 8 points on the abutments. The bored pile on the bridge's main span is 1.8 meters in diameter and 70 meters in length from the cut of level.

The bored piles are built in a location that has a 30 m soft soil layer from the surface. The soil at the project location is dominated by a soft soil layer. Soil investigation results show soil stratigraphy that consists of various types of consistency of the clay layer and a sand layer. The pile's end bearing is supported by a stiff clay layer rather than a hard soil layer. Analysis of pile capacity still uses assumptions and the correlation of soil parameters. One of them is the adhesion factor (α).

Determining skin friction capacity on bearing capacity of bored piles analysis is dependent on many factors between pile and soil. Over the years, many researchers have created equations for determining adhesion factors and they can prove them with analytical and numerical methods in their analysis [1]. The analysis demonstrates that the study can explain the effect of the adhesion factor and skin friction capacity in the clay layer.

Various adhesion factors depend on undrained shear strength (c_u) and construction method [2]. In stiff clay layer, Skempton [3] suggests 0.47 as α. That value is used in residual soil in Singapore [3]. The N_{SPT} value can be used to calculate pile friction (fs). Meyerhoft [4] suggests fs = 2N (kPa) for a driven pile in the sand. The equation is also used in residual soil in Singapore but at a pressure of no more than 120 kPa [5].

One of the methods used to determine the bearing capacity of bored piles is the bi–directional static loading test using the Osterberg Cell test. (OC test) method. The method was very effective in determining the bearing capacity of the bored pile on Suramadu Bridge [6]. It was found that the bored pile's bearing capacity did not meet the requirements. To increase the foundation's bearing capacity, a grouting was performed at the foundation's tip, followed by an OC test to determine its resistance after improvement.

Ideally, the friction resistance is determined from a systematic study of the load transfer characteristics obtained from the pile bearing capacity test equipped with a strain gauge along the pile. However, because this method is very expensive, the load transfer characteristics can be determined from tests in the same soil conditions [2].

Additionally, the number of piles tested is small, ranging between one and two [7–10]. Several researchers have conducted research on bored piles in soft to stiff clay soils with a load test and equipped with equipment so that the load transfer on the pile can be determined [2, 9–11]. The correlation between the parameters obtained in the field and the relevant soil conditions can be used to improve the design of the bored pile in the future [2]. The results obtained are compared between the bearing capacity calculated by empirical equations and also testing in the field.

Besides analytical methods, numerical study with finite element methods is also used in any case of soil-pile interaction. Some researchers use PLAXIS 2D for learning about pile behavior [7, 11–15]. The aim of this study was to use both analytical and numerical methods to determine the adhesion factors of soft to stiff clay.

II. LITERATURE REVIEW

According to Kiprotich [11], a foundation is basically a long structural element that transfers load from the upper structure through compressible soil (soft soil) to a more suitable material, like rock or stiff soil. If the hard soil layer is too deep, pile foundations are one of the deep foundations used to support the upper structure. This foundation is used to support the structure with an uplift force. The use of a deep foundation has the following advantages:

a. To transfer structure -load which located on water or soft soil layer to hard soil layer.

b. To transfer load to soft soil until a certain depth, the foundation can use a friction soil pile to keep the load transferred and supported.

c. To give resistance force that is affected by uplift forces caused by hydrostatic pressure.

d. To withstand horizontal and inclining forces,

e. To protect the foundation of the structure from surface water erosion.

Besides that, a large bored pile foundation can also be used as an energy pile that functions as a heating or cooling building system [16].

Based on load transfer from the upper structure, the pile foundation has 3 types of foundation:

a. Pile foundation with end bearing pile. This pile will support the supported soil layer by passing some of the upper structure load through the end-bearing point.

b. Pile foundation with friction pile. This pile will progress to an upper structure load through skin friction of the pile.

c. The combination of end bearing and skin friction.

The pile foundation generally consists of a bored pile, precast pile, steel pipe pile, timber pile, and a composite pile. Bored pile construction demands temporary steel casing of at least 15 m and bentonite as protection from sliding. Soil disturbance can occur when a cylinder is pulled out while the concrete is being poured. Because of that, in calculating the pile capacity in the sand layer, Tomlinson [17] suggests using the angle of friction from disturbing the sample, except if the pile is set on gravel.

The effect of bored piles installation on the adhesion factor between the pile and the soil surrounding the pile was studied, and it was discovered that the adhesion factor is lower than the undrained shear strength before pile installation. The stability of the soil in the vicinity of the bored hole may be the cause of this problem. When pouring concrete, water ground flows into a low-pressure zone in the vicinity of the borehole, increasing soil pliability. If boring and pouring are done in one or two hours, the soil meets requirements will be reduced [18]. The base condition was also affected by the bore hole, resulting in increased settlement.

Many researchers, including Reese and Wright [19], Meyerhoff [20], and Terzaghi and Peck [21], have found a correlation between N_{SPT} and pile capacities, but the pile capacity results are too conservative. Bowles [22] was supposed to increase Meyerhoff theory's allowable pile capacity by 50%.

The general equation for determining pile capacity, which is derived from total end bearing capacity and skin friction capacity, is:

$$Q_u = Q_p + Q_s - W_p \quad (2.1)$$

where Q_u = ultimate total pile capacity (ton), Q_p = ultimate bearing capacity (ton), Q_s = ultimate shear friction capacity (ton), and W_p= pile weight (ton).

Equation 2.2 is used to calculate the end bearing pile capacity of cohesive soil. Equation 2.3 can be used to calculate the end bearing pile capacity per unit area qp in cohesive soil. Furthermore, Reese and Wright [19] shows a correlation between q_p and N_{SPT} in non-cohesive soil.

$$Q_p = Ap.q_p \quad (2.2)$$

$$q_p = 9.c_u \quad (2.3)$$

$$c_u = 2/3.N_{SPT} \quad (2.4)$$

where Q_p = Ultimate end beading pile capacity (ton), A_p = bored pile Area (m^2), q_p = end bearing capacity per unit area (ton/m), and c_u = Undrained shear strength (ton/m^2).

Moreover, skin friction pile capacity can be calculated using Equation 2.5.

$$Q_s = f.\ Li.\ p \quad (2.5)$$

where f = skin friction per unit area (ton/m^2), Li = layer length (m), and p = circumference of pile (m), and Qs = ultimate skin friction capacity (ton).

For cohesive soil, the skin friction per unit area can be calculated using Equation 2.6.

$$f = \alpha.\ c_u \quad (2.6)$$

where α = adhesion factor and c_u = indrained shear strength (ton/m^2).

According to the Reese and Wright [19] Method, α = 0.55 for cohesive soil. And, for non-cohesive soil, friction resistence can be obtained from a correlation with N_{SPT}. Moreover, using the Kulhaway [23] method, it can be determined from the undrained shearing resistance vs adhesion factor graph. Another method, Resse and O'Neil [24], reported the adhesion factor as a function of undrained shear strength with a range as shown in Table 1.

Table 1 Adhesion Factor Reese and O'Neil [24]

c_u kN/m^2	α
< 191.52	0.55
191.52 – 287.28	0.49
287.28 – 383.04	0.42
383.04 – 478.80	0.38
478.80 – 574.56	0.35
574.56 – 670.32	0.33
670.32 – 766.08	0.32
766.08 – 861.84	0.31
861.84	*As rock*

Following that, various adhesion factors are obtained from Cerruibini and Vesia [1], and the reported adhesion factor data of Weltman and Healy [25] is digitized and is shown in the equation below.

$$\alpha = 83.54 C_u^{-1.032} \quad (2.7)$$

Then, validation of adhesion factor is adopted from Kulhawy & Jackson [26] method was gained from distribution data on 106 bored pile in which 41-piles of them were adjusted on compression test and 65-piles of them were adjusted on tensile test [1]. The result obtained is as Equation 2.8. Meanwhile, as shown in Table 2, Coduto [27] observed a relationship between Cu and alpha for bored and driven piles.

$$\alpha = 0.21 + 0.26\, Pa/c_u \quad (2.10)$$

Table 2 Correlation between α and c_u for Bored Piles and Driven Piles [27]

Type	Equation	Range
Bored piles	α	for $c_u \le 51$ kPa
Bored Piles	α	for $c_u > 51$ kPa
Driven Piles	α	for $c_u \le 32$ kPa
Driven Piles	α	for $c_u > 51$ kPa

Determining pile foundation capacity can be done using a field pile load test. And the data is analyzed using the Davisson and Chin methods. The following is the method suggested by Davisson [28].

a. Determine load vs settlement curve.
b. Determine elastic settlement that be calculated with below equation.

$$S_e = \frac{Q \times L}{A_p \times E_p} \quad (2.9)$$

Whereas S_e= elastic settlement (mm), q= load test (N), L= pile length (mm), A_p= area of pile (mm^2), and E= Modulus elasticity of soil (MPa).

c. Draw a line from (0,0) based on the elastic settlement equation.
d. Line 2 should be drawn parallel to line 1 at a distance of x, which can be calculated using the equation below.

$$x = 0.15 + \frac{D_{fondasi}}{120}\ (in) \quad (2.10)$$

The pile foundation capacity is defined as the intersection of the load-settlement curve and the straight line.

Chin's method [29, 30] is one of the methods frequently used to analyze ultimate pile capacity in loading tests. The ultimate pile capacity can be calculated in the following steps.

a. Draw ratio settlement/load vs settlement curve.
b. Draw a straight line to represent the data distribution, or use Excel to create a trendline.
c. Determine the gradient or inclined part of the linear equation.

The following equation can be used to calculate the ultimate load.

$$Q_{ultimit} = \frac{1}{a \times gradien} \quad (2.11)$$

Whereas the a value falls between 1.2 and 1.4.

III. METHODS AND PROCEDURES

To obtain data on soil parameters and stratigraphy at the site, eight drill points were used in the soil investigation. The soil data in BH4 (borehole) was closest to the bored pile under review (B7). Fig. 1 depicts the results of the SPT and soil layer tests in BH4. At a certain depth, undisturbed samples were also taken and tested in the lab. Table 3 summarizes the findings.

A bi-axial static loading test with a hydraulic mechanism running parallel to the load was used. A load cell was installed in bored pile reinforcement as part of the foundation, and it works in two directions (bi-directional): upward (to resist skin friction and pile foundation weight) and downward (to resist pile foundation weight) (to resist of skin friction and end-bearing). The load cell was placed at a depth of 42 meters (Fig. 1). Both resistances in a part are automatically recorded by a load cell. The term "load cell" refers to the reactions that take place on a bored pile foundation. When the soil parameter and tools reached their maximum load, the loading test was stopped. Bi-axial loading tests were conducted in the field with B7 pile. Table 4 summarizes the pile data.

The empirical methods of gaining an interpretation of pile capacity results were used in the back–calculation analysis to obtain the adhesion factor. Back–calculation was performed using the empirical equations according to the pile foundation theory (Table 5). To represent the position and validate this calculation, the adhesion factor's result is plotted and compared with other adhesion factors obtained by other researchers.

The finite element method is used to create a bored pile foundation model in the final stage. The PLAXIS 2D computer program was used in the FEM model. PLAXIS 2D is now the most widely used software for creating FEM models [31]. the program was used to build a pile foundation model and soil layer by analyzing pile capacity and settlement using the finite element method. Asymmetry was used as the analysis model. The elements used in the final product were desirable.

With 50 m-horizontal axes, a geometry model was created up to a depth of 100 meters. The geometry of the material was determined using field and laboratory data. Axisymmetric modeling was used to generate the foundation (Fig. 2). The soil model was created using the Mohr–Coulomb model with data summarized in Table 6. Furthermore, the concrete used was linearly elastic and non-porous in nature. The settlement as a function of load was the subject of the results of the analysis. As a result, the outcome was used to calculate the ultimate load-settlement curve, which was then compared to the field load test obtained from the bi-axial test. Data that was not obtained in this study, such as the soil's modulus of elasticity and Poisson's ratio, was taken from the literature, as shown in Table 7.

Table 3. Soil samples laboratory test results

No	Location of Sample	Depth of Sample (m)	Sample Type	USCS	Spesific Gravity	IP (%)	Gravel (%)	Sand (%)	Silt (%)	Clay (%)
1	BH - 4	27 - 27.3	DS	SC	2.66	11.21	0	67.79	23.53	8.69
2	BH - 4	33 - 33.3	DS	SW	2.667	-	0	97.74	2.27	
3	BH - 4	38 - 38.3	DS	SW	2.678	-	0	98.84	1.17	
4	BH - 4	43 - 43.3	DS	SW	2.677	-	0	97.68	2.33	
5	BH - 4	48 - 48.3	DS	CH	2.617	61.09	0	0.56	40.1	59.35
6	BH - 4	59 - 59.3	DS	CH	2.653	67.13	0	0.2	43.86	55.93
7	BH - 4	73 - 73.3	DS	CH	2.59	72.35	0	0.16	54.31	45.53
8	BH - 4	93 - 93.3	DS	CH	2.642	74.16	0	0.13	48.79	51.09

Table 4. Bored pile foundation data of B7

Pile No.	Diameter	G.L Elevation	COL Elevation	Total Length	Bor Log	GeoCell Elevation	Test Load	GeoCell Depth Location
	mm	m	m	m		m	Ton	m
B7 West Pylon	1800	13.354	11.131	73.336	BH-04	-28.646	2x900	42

Table 5 Back-calculation equation on Upward and Downward

No.	Depth	Position	Equation
1	0-42	Upward	$Q_{upward} = \Sigma Q_{s,\,clay}$
			$Q_{s,clay}$
			$Q_{s,sand}$
2	42-73	Downward	$Q_{downward} = Q_p + \Sigma Q_{s,\,clay} + \Sigma Q_{s,\,sand}$
			Q_p
			$Q_{s,clay}$
			$Q_{s,sand}$

Table 6. Soil properties used in finite element analysis

Bore Hole ID	Depth (m)	Soil Type	Nspt	γ_n kN/m³	γ_{sat} kN/m³	E kN/m²	ν	c_u kN/m²	ϕ (˚)
BH - 04	0 - 15	Very Soft Clay	2	14.67	16.13	3106.67	0.30	10	-
	15 - 25	Soft Clay	3	15.33	16.87	4143.33	0.40	15	-
	25 - 30	Loose Sand	5	13.78	15.16	16483.33	0.29	-	28.1
	30 - 48	Medium Dense Sand	25	16.95	18.64	24876.32	0.36	-	33.9
	48 - 67	Medium Clay	12	17.33	19.07	8626.67	0.40	60	-
	67 - 100	Stiff Clay	24	19.56	21.51	22616.67	0.47	120	-

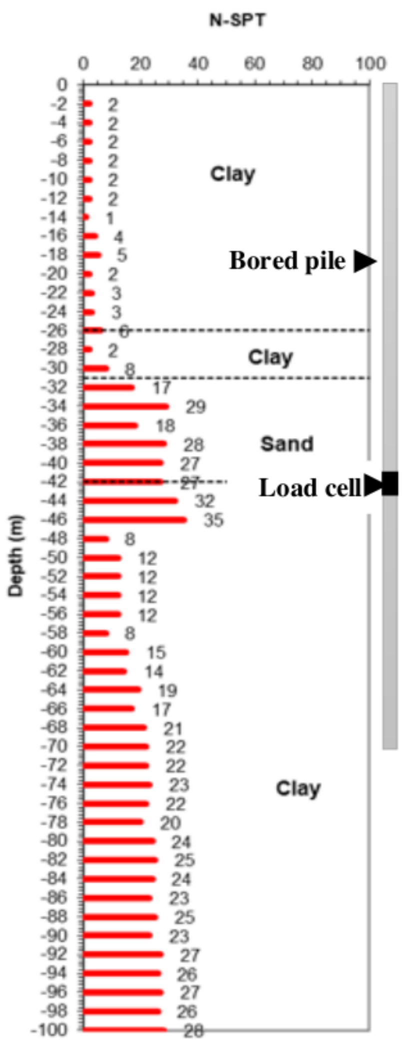

Fig. 1 Soil stratigrafi and N_{SPT} data

Table 7. Soil's Modulus Elasticity and Poisson's ratio based on soil type [32]

Type of Soil	E_s MN/m²	Poisson's ratio, μ_s
Loose sand	10.35 - 24.15	0.2 - 0.4
Medium dense sand	17.25 - 27.60	0.25 - 0.4
Dense sand	34.50 - 55.20	0.30 - 0.45
Silty sand	10.35 - 17.25	0.20 - 0.40
Sand and gravel	69.00 - 172.50	0.15 - 0.35
Soft clay	2.07 - 5.18	0.20 - 0.50
Medium clay	5.18 - 10.35	
Stiff clay	10.35 - 24.15	

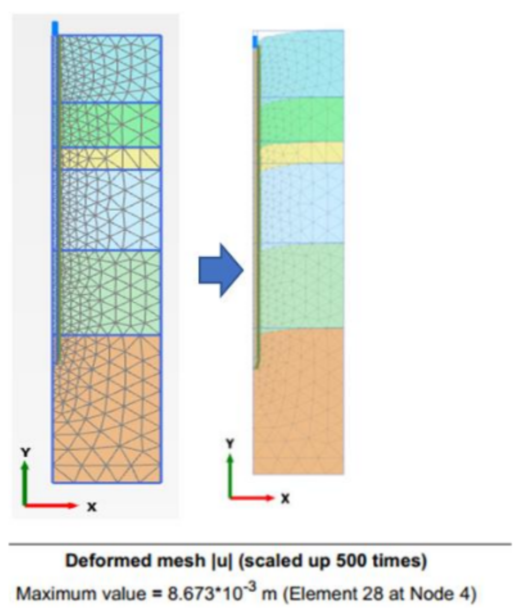

Fig. 2. Mesh generate model and an example result of Plaxis

III. RESULTS AND DISCUSSIONS

The field test results from the B7 pile loading test are shown in Table 7. The data was then plotted on a graft, as shown in Fig. 3. Both upward and downward deformation data were analyzed as a single curve. Table 7 shows the final result. Davisson and Chin methods were used to determine the pile's bearing capacity, as shown in Fig. 3 and 4. The bearing capacity of the pile was analyzed using Davisson and Chin methods.

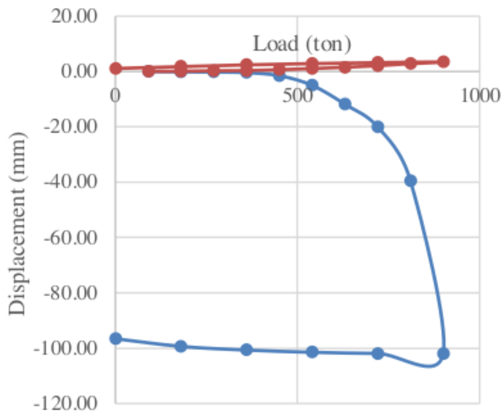

Fig.3. Load-Displacement Curve of B7 is Both of Downward and Upward Position

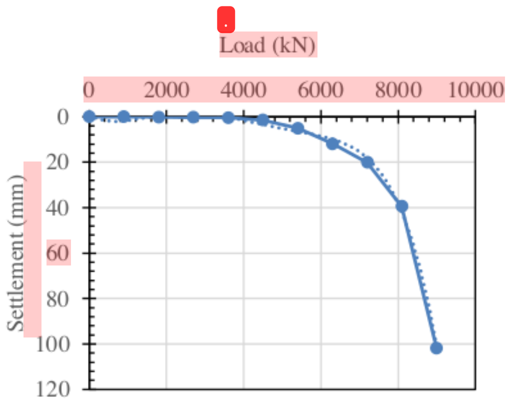

Fig. 4 Downward Load Displacement of B7

A. Chin's Method

Determining the ultimate load with the chin method can be obtained at some stages, i.e.

a. Tabulate the data that will be analyzed and display it in Table 8.

b. Draw a scattered graph with y-coordinates as settlement/load and x-coordinates as settlement.

c. Create trendline linear and equation plotting data distribution. Fig. 5 and 6 show the data in upward and downward positions.

d. Equation 2.11 was used to calculate the ultimate load from the bored pile using the gradient of the trendline equation.

Table 8 Bored Piles Test Result of B7

Load	Load	Downward Displacement (mm)	
2×kN	2×ton	Current Grade	Cummulative Displacement
0	0	0	0
900	90	0.00	0.00
1800	180	0.10	0.10
2700	270	0.11	0.21
3600	360	0.21	0.42
4500	450	1.10	1.52
5400	540	3.48	5.00
6300	630	6.83	11.83
7200	720	8.21	20.04
8100	810	19.45	39.49
9000	900	62.47	101.96

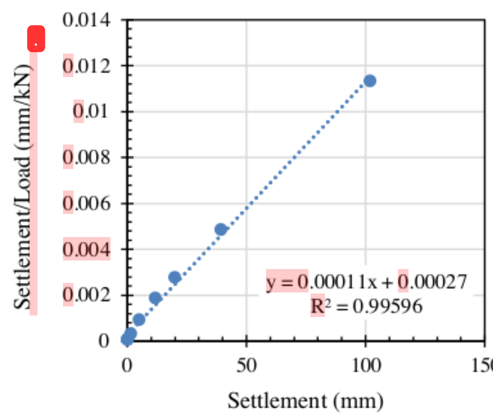

Fig. 5 Interpretation Results of Downward Load Displacement Curve of B7 Piles with Chin's Method

B. Davisson's Method

The Davisson method can be used to calculate the ultimate load at various stages, i.e.

a. Tabulate the data will be analyzed that can be present such as Chin's method data.

b. Determine elastic settlement using Equation 2.9.

c. Draw a linear line based on the elastic settlement occurring.

d. Determine the x distance and draw a parallel shifting line (line 2) with Equation 2.10.

e. Draw a vertical line straight to the x coordinate from the intersection between Line 2 and the load vs settlement curve. The outcomes are depicted in the Fig. 7.

The bearing capacity of the pile is taken at the smallest value of the two methods. Using back–calculation using empirical equations as shown in Table 5, the adhesion factor was obtained and summarized in Table 9.

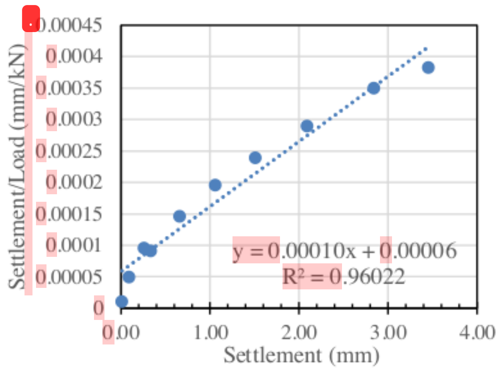

Fig. 6. Interpretation Results of Upward Load Displacement Curve of B7 Pile using Chin's Method

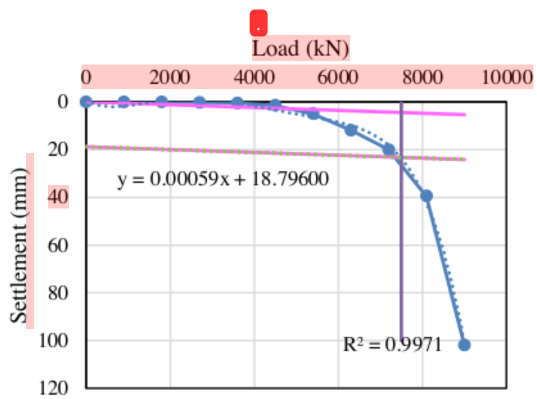

Fig. 7 Downward Load Interpretation of B7 Piles with Davisson's Method

Table 9 Adhesion factor result of B7

Qu Pakai (kN)		Metode	α average
Upward	8000.00	*Chin's*	0.943
Downward	7272.73	*Chin's*	0.191

The adhesion factor results from back-calculation analysis via adhesion factor from literatures are then checked. The data for this analysis comes from Kulhawy & Jackson [26], Coduto [27], and Weltman & Healy [28]. Kulhawy and Jackson [26], in which the graph shows adhesion factor results from back-calculation analysis, were used to compare the approached adhesion factor results in Fig. 8. The upward position of the adhesion factor indicated a soft soil layer, whereas the downward position indicated a hard soil layer.

In Fig. 9, the approached adhesion factor is based on Coduto [27], and the graph shows that the adhesion factor obtained through back-calculation analysis is comparable to the adhesion factor of the upward position rather than the downward condition. Similar to the previous figure (Fig. 10), the upward layer's adhesion factor is soft soil, while the downward layer's adhesion factor is stiff clay layer. In Fig. 10, the approach to the adhesion factor is based on the Cerrubini and Vesia [1] analysis, which represents the adhesion factor results from Weltman and Healy [25]. The curve in the figure depicts the adhesion factor of soft clay, which is determined by back-calculation close to the trendline rather than stiff clay.

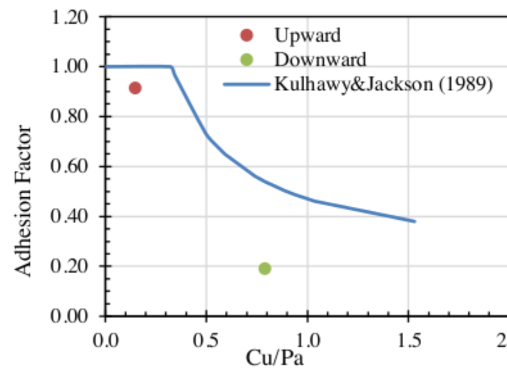

Fig. 8 Correlation between α and C_u/P_a for Bored Pile (Kulhawy and Jackson) [26]

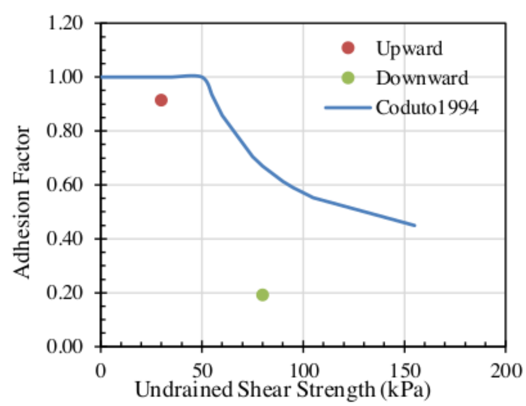

Fig. 9 Undrained Shear Strength vs α for Bored Pile (Coduto) [24]

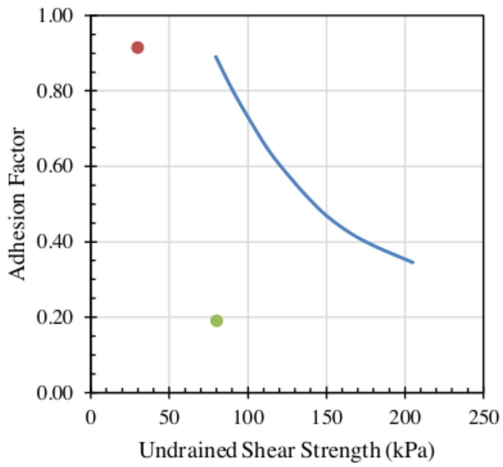

Fig. 10 Various Adhesion factor for Piles of B7 (Weltman and Healy 1978) [25]

The three approaches all produced the same trend, with the adhesion factor in the upward section closely matching the published data. While in the downward position, the obtained adhesion factor is still significantly less than the commonly used value. This is because, in the upward position, only skin friction supports and analyzes the pile. While the downward section includes an end resistance, some of the parameters used are still approximations.

Three approaches to adhesion factor position are obtained through back-calculations close to the data distribution of Kulhawy and Jackson's adhesion factor data [26]. Thus, the results obtained demonstrate that bearing capacity analysis will produce accurate results when Kulhawy and Jacson's [26] adhesion factor data is applied to the project location.

C. Plaxis Analysis

PLAXIS Connect Edition was used for numerical analysis. Fig. 11 illustrates the equivalent top load-settlement model result. The graph from the PLAXIS 2D model is shown to be close to the field results based on the model results obtained in the figure. As a result, it can be interpreted as a conclusion regarding the soil parameters used. The friction coefficient determined by the PLAXIS Model was then used to calculate the adhesion factor in the interaction of the bored pile section with the clay layer. The obtained adhesion factor is then plotted against the adhesion factor distribution data from Kulhawy and Jackson [26], Coduto [27], and Weltman & Healy [25].

According to Fig.s 12–14, adhesion factors obtained using PLAXIS 2D Modelling conform to the adhesion factor data proposed by Kulhawy and Jackson [26], Coduto [27], and Weltman and Healy [25]. This instance bears some resemblance to empirical adhesion factors, such as those depicted in Fig. 12. The results obtained can then be used to demonstrate that bearing capacity analysis is accurate when Kulhawy and Jacson's [26] adhesion factor data is used. Additionally, the result indicates that the adhesion factor calculated using this finite element is more consistent with published data. This is because finite element modeling allows for the distribution of bearing capacity contributions, particularly in the downward portion between skin friction and end bearing analysis.

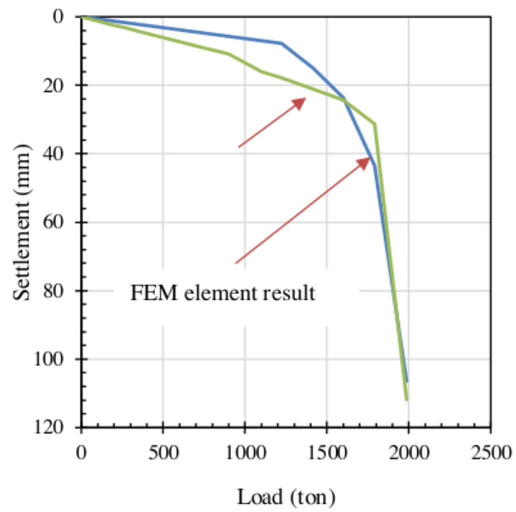

Fig. 11 Equivalent Curve Top Load – Settlement from PLAXIS 2D

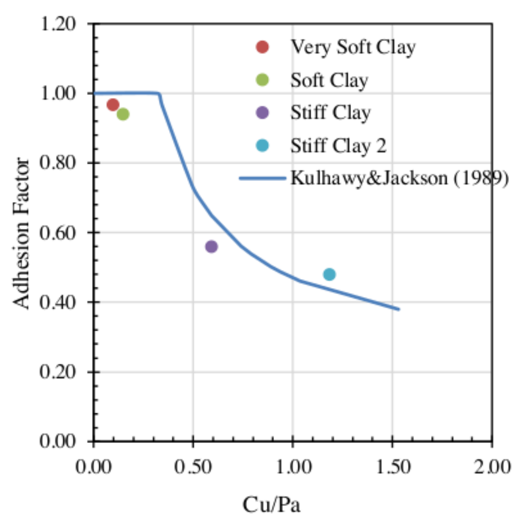

Fig. 12. Distribution Data of Adhesion Factor from Output PLAXIS through Adhesion Factor of Kulhawy and Jackson data [26]

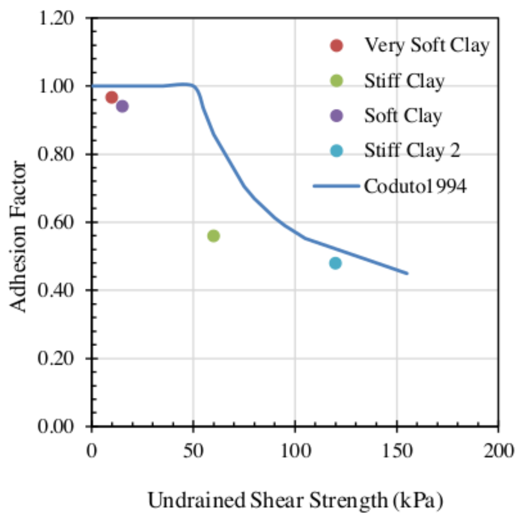

Fig. 13 Distribution Data of Adhesion Factor from Output PLAXIS through Data of Coduto [27]

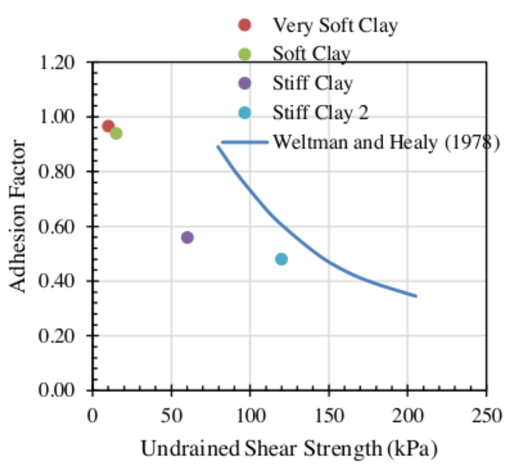

Fig. 14 Distribution Data of Adhesion Factor from Output PLAXIS through Adhesion Factor of Weltman and Healy data [25]

V. CONCLUSIONS

Back-calculation was used to calculate an adhesion factor based on the interpretation of the pile's load capacity, both upward and downward.The average adhesion factor obtained is 0.943 upward and 0.191 downward on Piles of B7. The adhesion factor result was compared with the adhesion factor curve of the other adhesion factor data. Back-calculation has resulted in close to the distribution data of the Kulhawy and Jackson (1989) data. PLAXIS 2D Modeling also generates adhesion factors of 0.97 and 0.94 in very soft clay and soft clay layers, respectively, as well as 0.56 and 0.48 in stiff clay and very stiff clay. These adhesion factor distributions are similar to those reported by Kulhawy and Jackson (1989) and Coduto (1989).

REFERENCES

[1] C. Cherubini, G. Vessia, Reliablity approach for the side resistance of piles by means of the total stress analysis (α Method). Can. Geotech. J. 44 (2008) 1378-1390. doi:10.1139/t07-061

[2] M.F. Chang, and B.B. Broms, Design of bored piles in residual soils based on field-performance data. Canadian Geotechnical Journal. 28(2) (1991) 200–209. doi:10.1139/t91-027

[3] A.W. Skempton, Cast in-situ bored piles in London clay. Geotechnique. 9 (1959) 153-157.

[4] G.G. Meyerhof, The bearing capacity and settlements of pile foundations. ASCE Journal of the Geotechnical Engineering Division. 102(GT3) (1976) 197-228.

[5] B.B. Broms, M.F. Chang, and A.T.C. Goh, Bored piles in residual soils and weathered rocks in Singapore. Proceedings of the 1st International Geotechnical Seminar on Deep Foundations on Bored and Auger Piles, Ghent, Belgium, (1988) 17-34.

[6] M. Irsyam, A. Sahadewa, A Boesono, S. Soebagyo. Pengaruh Strength Reduction Tanah Clay – Shale Akibat Pelaksanaan Pemboran Terhadap Nilai Daya Dukung Pondasi Tiang di Jembatan Suramadu Berdasarkan Hasil Tes OC. Jurnal Teknik Sipil. 4(2) (2007) 69-92. https://doi.org/10.5614/jts.2007.14.2.1

[7] M. Ezzat, Y. Zaghloul, T. Sorour, A. Hefny, M. Eid, Numerical Simulation of Axially Loaded to Failure Large Diameter Bored Pile. International Journal of Geotechnical and Geological Engineering. 13(5) (2019) 283-297.

[8] G. Gao, M. Gao, Q. Chen, J. Yang. Field Load Testing Study of Vertical Bearing Behavior of a Large Diameter Belled Cast-in-Place Pile. KSCE Journal of Civil Engineering. 23 (2019) (2009–2016).

[9] G. Dai, R. Salgado, W. Gong, and Y. Zhang. Load tests on full-scale bored pile groups. Can. Geotech. J. 49 (2012) 1293–1308.

[10] Q.Q. Zhang, Z.M. Zhang, S.C. Li. Investigation into Skin Friction of Bored Pile Including Influence of Soil Strength at Pile Base. Marine Georesources & Geotechnology. 31(1) (2013) 1-16 DOI: 10.1080/1064119X.2011.626506

[11] N. Kripotich, Modelling of Negative Skin Friction on Tiang Bor in Clay. Chalmers University of Technology. Sweden. (2015).

[12] M. Eid , A. Hefny, T. Sorour, Y. Zaghloul, M. Ezzat. Full-Scale Well Instrumented Large Diameter Bored Pile Load Test in Multi Layered Soil: A Case Study of Damietta Port New Grain Silos Project. International Journal of Current Engineering and Technology. 8(1) (2018) 85-92.

[13] M. Hol'ko, J. Stacho. Comparison of Numerical Analyses with a Static Load Test of a Continuous Flight Auger Pile. Slovak Journal of Civil Engineering. 22(4) (2014) 1-10.

[14] P.J. Vardanega, M.G. Williamson, M.D. Bolton. Bored pile design in stiff clay II: mechanisms and uncertainty. Proceedings of the Institution of Civil Engineers: Geotechnical Engineering 165. (2015) 233-246. http://dx.doi.org/10.1680/geng.11.00063.

[15] R.P. Cunha, A.F.B. Cordeiro, M.M. Sales, Numerical assessment of an imperfect pile group with de-fective pile both at initial and reinforced conditions.Soils and Rocks. 33(2) (2010) 81-93.

[16] W. Ounaies, Geotechnical Impacts of Energy Piles. IJCE. 6(2) (2019) 1-3 doi: 10.14445/23488352/IJCE-V6I2P101

[17] M.J. Tomlinson. Pile design and construction practice. Seventh Edition. Pearson education limited. (2001).

[18] D.J. Palmer, R. Holland, The Construction of Large Diameter Bored Piles with Particular Reference to Londo n Clay, Proceedings Conference on Large Bored Piles, ICE, London, (1966) 105- 120.

[19] L.C. Reese, and S.J. Wright, Drilled Shaft Manual-Construction Procedures and Design for Axial Loading, Vol. 1, U.S. Dept. of Transportation, Implementation Division, HDV-22, Implementation Package. (1977) 77-21.

[20] G.G. Meyerhof, Generai Report : Outside Europe, Proceedings

Conference on Penetration Testing, Stockholm. 2 (1974) 40-48.
[21] K. Terzaghi, and R. B. Peck. Soil Mechanics in Engineering Practice. 2nd ed., John Wiley & Sons, Inc., New York. (1967) 729 pp.
[22] J.E. Bowles. Foundation analysis and design. Mcgraw-Hill International Book Company. 3rd Edition. (1982)
[23] F.H. Kulhawy. Limiting Tip and Side Resistance-Fact or Fallacy, Analysis and Design of Pile Foundations, ed. J.R. Meyer, ASCE, New York, N.Y. (1984) 80-98.
[24] L.C. Reese, and M.W. O'Neill, Drilled Shafts: Construction Procedures and Design Methods, FHWA Publication No. FHWA-JI-88-042 atau ADSC Publication No. ADSC-TL-4, August. (1988) 564.
[25] A.J. Weltman, and P.R. Healy. Piling in boulder clay and other glacial tills. Construction Industry Research and Information Association, Report PG5. (1978).
[26] F.H. Kulhawy, and C.S. Jackson. Some observations on undrained side resistance of drilled shafts. Foundation Engineering: current principles and practices Congress Evanston Illinois. 2 (1989) 1011–1025.
[27] D.P. Coduto. Foundation design, principles and practices. Prentice Hall Inc., Englewood Cliffs, N.Y. (1984).
[28] M.T. Davisson, High Capacity Piles. Proceedings, Lecture Series, Innovations in Foundation Construction, ASCE, Illinois Section, Chicago, March 22, (1972) 81-112.
[29] F.K. Chin. Estimation of the ultimate load of piles from tests not carried to failure. Proceedings of the Second Southeast Asian Conference on Soil Engineering, (1970) 83-91.
[30] F.K. Chin. The inverse slope as a prediction of ultimate bearing capacity of piles, Proceedings 3rd Southeast Asian Conference on Soil Engineering. (1972) 83-91.
[31] Plaxis. General Information Manual: Connect edition V21.01. Bentley. 2021.
[32] B.M. Das. and K. Sobhan. Principles of Geotechnical Engineering. Ninth Edition, USA : Cengage Learning. (2018).

Adhesion Factor of Large Diameter Bored Piles in Soft to Stiff Clay in the Sei Alalak Bridge Replacement Project–South Kalimantan, Indonesia

ORIGINALITY REPORT

11%	7%	8%	4%
SIMILARITY INDEX	INTERNET SOURCES	PUBLICATIONS	STUDENT PAPERS

MATCH ALL SOURCES (ONLY SELECTED SOURCE PRINTED)

3%

★ Jialin Zhou, Erwin Oh. "Full-Scale Field Tests of Different Types of Piles", Springer Science and Business Media LLC, 2021

Publication

Exclude quotes	On	Exclude matches	Off
Exclude bibliography	On		